

Cite this: *Phys. Chem. Chem. Phys.*, 2011, **13**, 7295–7297

www.rsc.org/pccp

## Exploring the thermochromism of sulfite-embedded polyoxometalate capsules†

Ryo Tsunashima,<sup>a</sup> De-Liang Long,<sup>a</sup> Toru Endo,<sup>b</sup> Shin-ichiro Noro,<sup>bc</sup> Tomoyuki Akutagawa,<sup>bc</sup> Takayoshi Nakamura,<sup>bc</sup> Raul Quesada Cabrera,<sup>d</sup> Paul F. McMillan,<sup>d</sup> Paul Kögerler<sup>e</sup> and Leroy Cronin<sup>\*a</sup>

Received 9th January 2011, Accepted 17th February 2011

DOI: 10.1039/c1cp20074g

The Dawson-type polyanion  $[\alpha\text{-Mo}_{18}\text{O}_{54}(\text{SO}_3)_2]^{4-}$ , with two  $\text{SO}_3^{2-}$  templates embedded inside a polyoxomolybdate(vi) cage, exhibits thermochromism over an exceptionally wide temperature range ( $\sim 500$  K). The temperature dependence of the cluster structure, established from X-ray crystallography, IR and Raman spectroscopy and DFT calculations, is related to a decreasing HOMO–LUMO gap in the near UV with increasing temperature. We postulate this is due to geometrical changes that affect both the occupied and unoccupied frontier molecular orbitals of this cluster anion.

The field of polyoxometalate (POM) chemistry is currently undergoing a vast transition with a shift of focus from structure to functionality,<sup>1–7</sup> a development in part motivated by the large degree of variability of key POM characteristics, *e.g.* redox activity, flexible structures, solubility and nanosized structures. We have pursued POM functionalization *via* the integration of electronically interesting groups into classical POM architectures and have to this effect isolated the  $\{\text{M}_{18}\}$  Dawson derivatives  $\alpha$ - and  $\beta$ - $[\text{Mo}^{\text{VI}}_{18}\text{O}_{54}(\text{S}^{\text{IV}}\text{O}_3)_2]^{4-}$  integrating two sulfite moieties.<sup>8–10</sup> The corresponding salts with tetraalkylammonium counterions exhibit thermochromism, namely a reversible pale yellow-to-red colour change upon heating from 77 to 500 K (Fig. 1).<sup>9</sup> An unusual electronic interaction between the encapsulated sulfite groups furthermore is evident from temperature-dependent intramolecular redox transitions these clusters undergo on metallic surfaces, a process linked to the partial formation of dithionate ( $\text{O}_3\text{S}-\text{SO}_3^{2-}$ ).<sup>10,11</sup>

<sup>a</sup> WestCHEM, Department of Chemistry, University of Glasgow, Joseph Black Building, University Avenue, Glasgow G12 8QQ, UK. E-mail: l.cronin@chem.gla.ac.uk; Fax: +44 (0)141 330 4888

<sup>b</sup> Graduate School of Environmental Science, Hokkaido University, Sapporo 060-0810, Japan

<sup>c</sup> Research Institute for Electronic Science, Hokkaido University, Sapporo 001-0020, Japan

<sup>d</sup> Department of Chemistry and Materials Chemistry Centre, Christopher Ingold Laboratories, University College London, London WC1H 0AJ, UK

<sup>e</sup> Institut für Anorganische Chemie, RWTH Aachen University, 52074 Aachen, Germany

† Electronic supplementary information (ESI) available: Crystallography and spectroscopic details. CCDC reference numbers 807474 and 807475. For ESI and crystallographic data in CIF or other electronic format see DOI: 10.1039/c1cp20074g

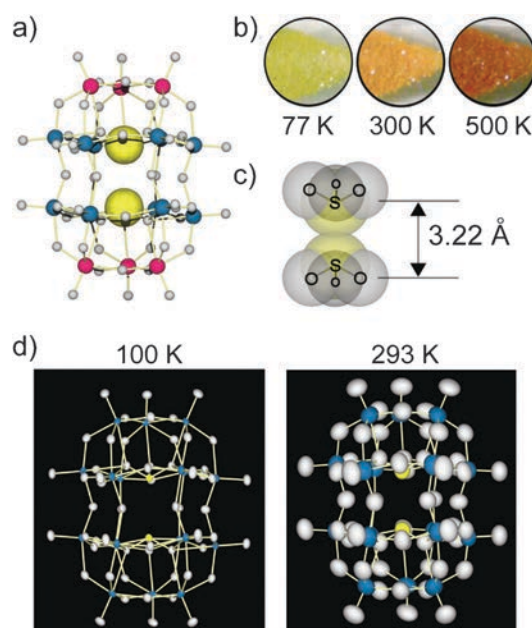


**Fig. 1** (a) Ball and stick representations of cluster **1a** (outer Mo pink, inner Mo blue, O grey, S yellow); (b) picture of single crystals at 77 K, 300 K and 500 K; (c) van der Waals radii of sulfite moieties in cluster **1a**. (d) Structure of **1a** in **1** at (a) 100 K and (b) 293 K with thermal ellipsoids of 80% probability (Mo blue, O white, S yellow).

We initially assigned the observed thermochromism to the structure–energy correlation of the frontier orbitals which are differently affected by the geometric changes induced by thermal vibrations.<sup>9</sup> Whereas in this initial description the sulfite-centred HOMOs are mostly unaffected by molecular vibrational modes, the lowest unoccupied molecular orbitals, localized on the polyoxomolybdate cage and primarily of Mo(4d) character, are susceptible to energy changes by *e.g.* breathing modes, causing a bathochromic effect at higher temperatures. The observed Vis absorption is then due to LMCT transitions involving internal sulfite ‘ligands’. Note that the eclipsed ( $\alpha$  isomer) arrangement of the sulfite groups with an S $\cdots$ S distance of 3.22 Å, *i.e.* significantly smaller than twice the van der Waals radius of sulfur, implies significant electronic interactions between the sulfur lone pairs. In addition, the

average Mo–O bond length involving sulfite oxo positions of 2.48 Å is longer than other Mo–O bonds (avg. 1.92 Å), suggesting that two sulfite moieties are loosely embedded with weaker Mo–O bonds, which is more conducive towards thermal displacement of the S positions.

Since thermochromism is sometimes governed by very small changes of the electronic/physical structure, detailed analysis and characterisation can be challenging. For example, the well-known thermochromic salicylideneanilines have been investigated for 40 years.<sup>12,13</sup> In order to establish a more detailed mechanism for the observed thermochromism, we isolated the  $[\alpha\text{-Mo}^{\text{VI}}_{18}\text{O}_{54}(\text{S}^{\text{IV}}\text{O}_3)_2]^{4-}$  polyanion (**1a**) as  $(n\text{Bu}_4\text{N})_6[\alpha\text{-Mo}_{18}\text{O}_{54}(\text{SO}_3)_2][\text{Mo}_6\text{O}_{19}]$  (**1**) and  $(\text{Pn}_4\text{N})_4[\alpha\text{-Mo}_{18}\text{O}_{54}(\text{SO}_3)_2]\cdot\text{CH}_3\text{CN}$  (**2**) and performed temperature-dependent studies.

Single-crystal X-ray diffraction measurements at 100 and 293 K of **1** indicate that the overall  $\{\text{Mo}_{18}(\text{SO}_3)_2\}$  cluster geometry only changes minimally. While the S··S distance remains virtually unchanged (100 K: 3.224 Å, 293 K: 3.219 Å), the POM shell widens slightly. The average distance between the symmetry-related Mo positions increases from 9.246 Å (100 K) to 9.267 Å (293 K). The thermal parameters  $U_{ij}$  of the Mo, O, and S sites correspondingly increase approximately by a factor of 5 (Fig. 1, Table 1).

Fig. 2 shows IR spectra of **2** measured from 11 to 290 K. The cluster **1a** shows IR bands at 972, 902 and 784  $\text{cm}^{-1}$  which are assigned to Mo=O<sub>term</sub> (972  $\text{cm}^{-1}$ ), Mo–O<sub>c</sub>–Mo corner-sharing octahedra (902  $\text{cm}^{-1}$ ) and Mo–O<sub>e</sub>–Mo edge-sharing octahedra (784  $\text{cm}^{-1}$ ), where O<sub>t</sub>, O<sub>c</sub> and O<sub>e</sub> implies terminal O atoms, O of corner-sharing octahedra and edge-sharing octahedra, respectively (see ESI†).<sup>14</sup> The band at 1481  $\text{cm}^{-1}$  originates from the organic counter cations, and the bands tend to increase in absorbance and width with increasing temperature, while no shift of the band positions is observed,

**Table 1** Averaged thermal parameters ( $1/3\text{Tr}(U_{ij})$ ) of **1** for Mo, O and S

	Mo/Å <sup>2</sup>	O/Å <sup>2</sup>	S/Å <sup>2</sup>
100 K	0.00973	0.01296	0.00865
293 K	0.05348	0.05850	0.04367

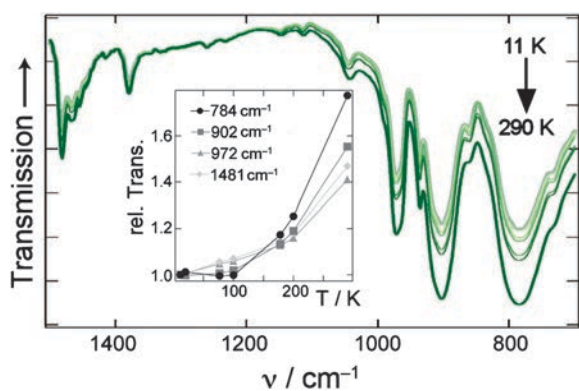


**Fig. 2** Temperature-dependent IR spectra of **2** from 11 K to 290 K (KBr pellets). Inset: relative transmission peak intensities for four bands as a function of  $T$ , normalized against intensities at 11 K.

**Table 2** Assignment of vibrational modes of **2** in IR and Raman spectra measured at 77 K and 293 K (wavenumbers in  $\text{cm}^{-1}$ )

	Mo=O + S–O <sub>s</sub> <sup>a</sup>		Mo–O <sub>c</sub> –Mo		Mo–O <sub>e</sub> –Mo		Mo–O <sub>s</sub> <sup>b</sup>
	$\nu_s$ Raman	$\nu_{as}$ IR/Raman	$\nu_s$ Raman	$\nu_{as}$ IR	$\nu_s$ Raman	$\nu_{as}$ IR	
77 K	995	972/971	902	902	620	784	246
293 K	992	972/968	902	902	620	784	242

<sup>a</sup> For solid  $\text{Na}_2\text{SO}_3$ , the symmetrical  $\nu_s(\text{S–O}_s)$  and the antisymmetrical  $\nu_{as}(\text{S–O}_s)$  modes appear at 990  $\text{cm}^{-1}$  and 952  $\text{cm}^{-1}$ , respectively. These bands here overlap with Mo=O bands. O<sub>c</sub>, O<sub>e</sub> and O<sub>s</sub> are defined in the text. <sup>b</sup> The assignment of this mode is only tentative due to coupling with lattice modes in this spectral region. Raman spectra were recorded using laser excitation wavelengths ranging from 477–780 nm minimising the incident power to minimise sample degradation.

see Fig. 2. The inset in Fig. 2 highlights the normalized intensity (referenced to intensities at 11 K) of the four main bands vs. temperature. We note different temperature dependencies of each vibration mode, with the band at 784  $\text{cm}^{-1}$  showing the most pronounced intensity increase with increasing temperature.

The Raman spectra of compound **2**, measured at 77 K and 293 K ( $\lambda_e = 544 \text{ nm}$ ), exhibit bands assigned to the polyanion **1a** that are compared to the corresponding IR bands in Table 2 (see ESI† for full spectra).<sup>14</sup> Raman shifts observed at 995  $\text{cm}^{-1}$ , 971  $\text{cm}^{-1}$ , and 246  $\text{cm}^{-1}$  at 77 K show bathochromic shifts of 3–4  $\text{cm}^{-1}$  upon heating to 293 K, though no significant shifts are observed for other bands. These three affected shifted bands involve sulfite-centred modes, indicating that Mo–O<sub>SO<sub>3</sub></sub> bonds are thermally responsive, compared to the Mo–O cage.<sup>14</sup>

In conjunction with these data we revisited our preliminary DFT calculations that were initially performed on the isolated polyanion **1a** in the gas phase. Because of the high charge of **1a**, this yielded an unreasonably small HOMO–LUMO separation of only 1.63 eV (corresponding to an absorption at 760 nm in the UV/Vis). In order to approximate the Madelung potential the polyanions experience in the solid-state structures of **1** and **2** we performed DFT calculations using the COSMO solvation model for an aqueous environment.<sup>15</sup> Using the crystallographic equilibrium coordinates for **1a** in **1**, this approach results in much more realistic energies of the frontier orbitals, with a HOMO–LUMO gap of 4.20 eV (295 nm) at 100 K and 4.16 eV (298 nm) at 293 K. Next to this small shift, we assign the origin of the thermochromism to a broadening effect of the primary HOMO–LUMO transition in the UV which causes an increasingly broad band to extend into the visible spectral region. Even though the S··S separation is virtually identical for both the 100 K and 293 K crystal structures, the slight expansion of the polyoxomolybdate shell allows for increased mobility and vibration amplitudes of the central S sites. This in turn results in a wider range of S··S interactions in the course of the S vibrations and in a variation of the energy of the highest occupied, sulfite-centred MOs. Together with a decrease in the energies of the lowest unoccupied MOs postulated earlier,<sup>9</sup> this effectively widens the HOMO–LUMO absorption band (Fig. 3a). Fig. 3b shows a schematic figure of the two S atoms inside **1a** as ellipsoids

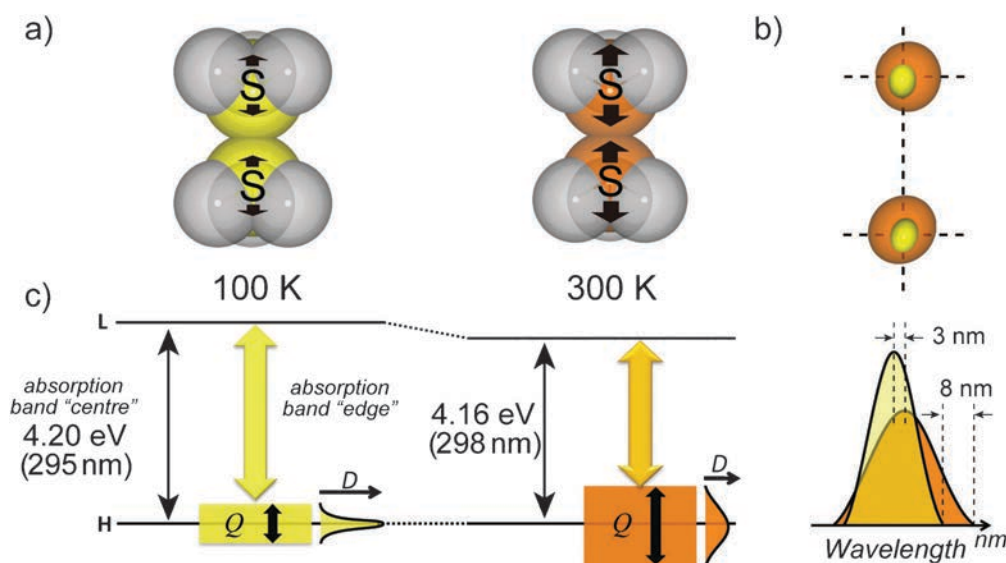


**Fig. 3** (a) Schematic representation of the thermal vibration of sulfite moieties shown as VDW models. (b) Comparison of two crystallographic anisotropic displacement ellipsoids (99% probability) for the sulfur sites at 100 K (yellow) and 293 K (orange). (c) Qualitative energy diagram of frontier orbitals next to HOMO (H) and LUMO (L) showing the splitting effect of the highest occupied, sulfite-centred molecular orbitals with increasing vibrational amplitudes.

with 99% probability. A wider spread of electron density ( $D$  in Fig. 3c) is observed at 293 K (orange) than that at 100 K (yellow). The vibrational displacement of the S atoms thus results in a wider absorption curve of the band spanned by the frontier orbitals. We estimate that the broadening  $Q$  is similar in quantity to the temperature difference (100 K  $\approx$  0.01 eV), implying a broadening by  $\sim 5$  nm from 100 K to 300 K. Diffuse reflection spectra at liquid nitrogen and room temperature which show a bathochromic shift of the absorption band edge of  $\sim 8$  nm (see ESI<sup>†</sup>), confirming the expected effects of both the HOMO–LUMO contraction due to equilibrium geometry changes and the estimated broadening  $Q$ .

## Conclusions

In summary, we postulate a semiquantitative mechanism for the thermochromism observed for tetraalkylammonium salts of the  $[\alpha\text{-Mo}_{18}\text{O}_{54}(\text{SO}_3)_2]^{4-}$  polyanion. The experimental shift of the HOMO–LUMO-centred absorption band by *ca.* 8 nm between 100 and 293 K appears to be linked to two primary factors: (a) a slight geometric expansion of the polyoxomolybdate cage with increasing temperature, causing a decrease in the energy of the lowest unoccupied molecular orbitals, and (b) a broadening of the energies of the highest occupied molecular orbitals due to increasing variations in the S–S distance of the S atoms embedded within the cluster cage. This finding highlights the potential of suitably functionalized polyoxomolybdates to provide intramolecular ‘electronic compartments’, a key requirement to redox switching functionality.

## Acknowledgements

We thank the EPSRC, WestCHEM and the University of Glasgow for supporting this work.

## Notes and references

- 1 A. Müller, F. Peters, M. T. Pope and D. Gatteschi, *Chem. Rev.*, 1998, **98**, 239.
- 2 C. L. Hill, *Chem. Rev.*, 1998, **98**, 1.
- 3 B. F. Hasenknopf, *Front. Biosci.*, 2005, **10**, 275.
- 4 D.-L. Long and L. Cronin, *Chem.–Eur. J.*, 2006, **12**, 3698.
- 5 D.-L. Long, E. Burkholder and L. Cronin, *Chem. Soc. Rev.*, 2007, **36**, 105.
- 6 P. Kögerler, B. Tsukerblat and A. Müller, *Dalton Trans.*, 2010, **39**, 21.
- 7 D.-L. Long, R. Tsunashima and L. Cronin, *Angew. Chem., Int. Ed.*, 2010, **49**, 1736.
- 8 C. Baffert, J. F. Boas, A. M. Bond, P. Kögerler, D.-L. Long, J. R. Pilbrow and L. Cronin, *Chem.–Eur. J.*, 2006, **12**, 8472.
- 9 D.-L. Long, P. Kögerler and L. Cronin, *Angew. Chem., Int. Ed.*, 2004, **43**, 1817.
- 10 C. Fleming, D.-L. Long, N. McMillan, J. Johnston, N. Bovet, V. Dhanak, N. Gadegaard, P. Kögerler, L. Cronin and M. Kadodwala, *Nat. Nanotechnol.*, 2008, **3**, 229.
- 11 C. Baffert, S. W. Feldberg, A. M. Bond, D. L. Long and L. Cronin, *Dalton Trans.*, 2007, 4599.
- 12 J. Harada, T. Fujiwara and K. Ogawa, *J. Am. Chem. Soc.*, 2007, **129**, 16216.
- 13 M. D. Cohen, G. M. J. Schmidt and S. Flavian, *J. Chem. Soc.*, 1964, 2041.
- 14 M. Fournier, R. Thouvenot and C. Rocchiccioli-Deltcheff, *J. Chem. Soc., Faraday Trans.*, 1991, **87**, 349; R. Thouvenot, M. Fournier, R. Franck and C. Rocchiccioli-Deltcheff, *Inorg. Chem.*, 1984, **23**, 598.
- 15 DFT single-point calculations employed TURBOMOLE 6.2 (O. Treutler and R. Ahlrichs, *J. Chem. Phys.*, 1995, **102**, 346), using standard TZVP basis sets and B3-LYP exchange functionals. No symmetry constraints were used.